

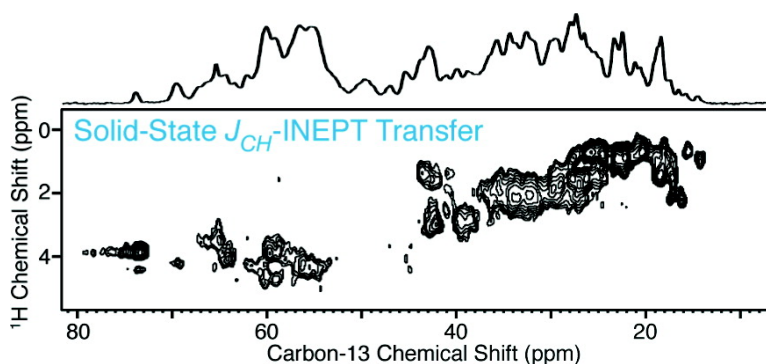
Article

## Proton to Carbon-13 INEPT in Solid-State NMR Spectroscopy

Bndicte Elena, Anne Lesage, Stefan Steuernagel, Anja Bckmann, and Lyndon Emsley

*J. Am. Chem. Soc.*, **2005**, 127 (49), 17296-17302 • DOI: 10.1021/ja054411x • Publication Date (Web): 18 November 2005

Downloaded from <http://pubs.acs.org> on March 25, 2009



### More About This Article

Additional resources and features associated with this article are available within the HTML version:

- Supporting Information
- Links to the 10 articles that cite this article, as of the time of this article download
- Access to high resolution figures
- Links to articles and content related to this article
- Copyright permission to reproduce figures and/or text from this article

[View the Full Text HTML](#)

## Proton to Carbon-13 INEPT in Solid-State NMR Spectroscopy

Bénédicte Elena,<sup>†</sup> Anne Lesage,<sup>\*†</sup> Stefan Steuernagel,<sup>‡</sup> Anja Böckmann,<sup>§</sup> and Lyndon Emsley<sup>\*†</sup>

Contribution from the Laboratoire de Chimie (UMR 5182 CNRS/ENS) Laboratoire de Recherche Conventionné du CEA (DSV 23V / DSM 0432) Ecole Normale Supérieure de Lyon, 69364 Lyon, France, Bruker BioSpin GmbH, Silberstreifen, 76287 Rheinstetten, Germany, and IFR 128 BioSciences Lyon-Gerland, Institut de Biologie et Chimie des Protéines UMR 5086 CNRS/UCBL, 7, passage du Vercors, 69367 Lyon, France

Received July 4, 2005; E-mail: Lyndon.Emsley@ens-lyon.fr; Anne.Lesage@ens-lyon.fr

**Abstract:** A refocused INEPT through-bond coherence transfer technique is demonstrated for NMR of rigid organic solids and is shown to provide a valuable building block for the development of NMR correlation experiments in biological solids. The use of efficient proton homonuclear dipolar decoupling in combination with a direct spectral optimization procedure provides minimization of the transverse dephasing of coherences and leads to very efficient through-bond <sup>1</sup>H–<sup>13</sup>C INEPT transfer for crystalline organic compounds. Application of this technique to 2D heteronuclear correlation spectroscopy leads to up to a factor of 3 increase in sensitivity for a carbon-13 enriched sample in comparison to standard through-bond experiments and provides excellent selectivity for one-bond transfer. The method is demonstrated on a microcrystalline sample of the protein Crh (2 × 10.4 kDa).

## 1. Introduction

Solid-state NMR of rare nuclei such as carbon-13 has developed through the widespread use of cross polarization (CP) and magic angle spinning (MAS), as well through the introduction of multidimensional correlation methods via through-space dipolar interactions.<sup>1</sup> However, through-bond scalar couplings are extremely valuable probes of direct proximities, and their use is an essential component in the assignment and characterization process of powdered solids. It has been shown that scalar couplings can be successfully resolved under MAS, and various techniques that employ *J* couplings in solids are currently applied for spectral editing<sup>2,3</sup> or acquisition of heteronuclear<sup>4,5</sup> or homonuclear<sup>6,7</sup> through-bond correlation spectra in both inorganic or organic solids.

In solution NMR, the INEPT technique is well-known as the method of choice for heteronuclear through-bond polarization transfer<sup>8,9</sup> and has become the cornerstone element of the great majority of multidimensional heteronuclear correlation experiments in use today for resonance assignment and structure determination by NMR. In solid-state NMR spectroscopy, the

INEPT technique was first introduced under MAS for through-bond transfers between weakly coupled nuclei in inorganic materials.<sup>10</sup> Conversely, the use of proton–carbon INEPT in solid samples has been limited to a few notable examples in the literature for either rather mobile systems, like cholesterol embedded in membranes,<sup>11</sup> or mesostructured silica-based particles.<sup>12</sup> Indeed, the rapid decay of transverse proton magnetization coherences in protonated crystalline solids has prevented until now any straightforward relevance of the <sup>1</sup>H–<sup>13</sup>C INEPT technique to NMR spectroscopy of ordinary organic powders. The effective transverse dephasing times of protons are very short for rigid crystalline solids,<sup>2,13</sup> where the dominant proton–proton dipolar couplings are not completely averaged

<sup>†</sup> Laboratoire de Chimie (UMR 5182 CNRS/ENS) Laboratoire de Recherche Conventionné du CEA (DSV 23V / DSM 0432) Ecole Normale Supérieure de Lyon.

<sup>‡</sup> Bruker BioSpin GmbH.

<sup>§</sup> IFR 128 BioSciences Lyon-Gerland, Institut de Biologie et Chimie des Protéines UMR 5086 CNRS/UCBL.

- (1) Laws, D. D.; Bitter, H. M. L.; Jerschow, A. *Angew. Chem., Int. Ed.* **2002**, *41*, 3096–3129.
- (2) Lesage, A.; Steuernagel, S.; Emsley, L. *J. Am. Chem. Soc.* **1998**, *120* (28), 7095–7100.
- (3) Sakellariou, D.; Lesage, A.; Emsley, L. *J. Magn. Reson.* **2001**, *151* (1), 40–47.
- (4) Lesage, A.; Sakellariou, D.; Steuernagel, S.; Emsley, L. *J. Am. Chem. Soc.* **1998**, *120* (50), 13194–13201.
- (5) Lesage, A.; Emsley, L. *J. Magn. Reson.* **2001**, *148* (2), 449–454.

- (6) Baldus, M.; Meier, B. H. *J. Magn. Reson.* **1996**, *121*, 65–69. Baldus, M.; Iulicci, R. J.; Meier, B. H. *J. Am. Chem. Soc.* **1997**, *119*, 1121–1124. Baldus, M.; Meier, B. H. *J. Magn. Reson.* **1997**, *128*, 172–193. Lesage, A.; Auger, C.; Caldarelli, S.; Emsley, L. *J. Am. Chem. Soc.* **1997**, *119*, 7867–7868. Verel, R.; Beek, J. D. v.; Meier, B. H. *J. Magn. Reson.* **1999**, *140*, 300–303. Chan, J. C. C.; Brunklaus, G. *Chem. Phys. Lett.* **2001**, *349*, 104–112. Olsen, R. A.; Struppe, J.; Elliott, D. W.; Thomas, R. J.; Mueller, L. J. *J. Am. Chem. Soc.* **2003**, *125*, 11784–11785. Mueller, L. J.; Elliott, D. W.; Leskowitz, G. M.; Struppe, J.; Olsen, R. A.; Kim, K. C.; Reed, C. A. *J. Magn. Reson.* **2004**, *168*, 327–335. Mueller, L.; Elliott, D. W.; Kim, K. C.; Reed, C. A.; Boyd, P. D. W. *J. Am. Chem. Soc.* **2002**, *124*, 9360–9361. Leppert, J.; Ohlenschlager, O.; Gorchach, M.; Ramachandran, R. *J. Biomol. NMR* **2004**, *29*, 167–173. Heindrichs, A. S. D.; Geen, H.; Giordani, C.; Titman, J. J. *Chem. Phys. Lett.* **2001**, *335*, 89–96. Hardy, E. H.; Verel, R.; Meier, B. H. *J. Magn. Reson.* **2001**, *148*, 459–464.
- (7) Lesage, A.; Bardet, M.; Emsley, L. *J. Am. Chem. Soc.* **1999**, *121*, 10987–10993.
- (8) Burum, D. P.; Ernst, R. R. *J. Magn. Reson.* **1980**, *39* (1), 163–168. Morris, G. A.; Freeman, R. *J. Am. Chem. Soc.* **1979**, *101* (3), 760–762.
- (9) Sorensen, O. W.; Ernst, R. R. *J. Magn. Reson.* **1983**, *51* (3), 477–489.
- (10) Fyfe, C. A.; Wongmoon, K. C.; Huang, Y.; Grondy, H. *J. Am. Chem. Soc.* **1995**, *117* (41), 10397–10398.
- (11) Soubias, O.; Reat, V.; Saurel, O.; Milon, A. *J. Magn. Reson.* **2002**, *158* (1–2), 143–148.
- (12) Alonso, B.; Massiot, D. *J. Magn. Reson.* **2003**, *163* (2), 347–352.
- (13) Elena, B.; De Paeppe, G.; Emsley, L. *Chem. Phys. Lett.* **2004**, *398* (4–6), 532–538.

by magic-angle spinning of the sample. Therefore both spectral editing techniques and two-dimensional (2D) heteronuclear correlation (HETCOR) methods employing  $J$  couplings, such as APT<sup>2</sup> or MAS-J-HMQC<sup>4</sup> experiments, have so far relied on a first step of cross-polarization to carbon, followed by edition or filtering of carbon transverse magnetization via heteronuclear  $J$  couplings. In these experiments the transverse component of the coherence is always on the carbon (or nitrogen) nucleus. While this leads to some useful experiments, this limitation rules out the use of INEPT based sequences and thereby eliminates all of the derivative multidimensional correlation experiments. This is a severe limitation on the development of solid-state NMR for microcrystalline proteins, for example.

Recent improvements of CRAMPS (combined rotation and multiple pulse spectroscopy<sup>14</sup>) techniques for averaging out proton homonuclear dipolar interactions, in particular with the development of a new generation of proton homonuclear dipolar decoupling schemes, such as the eDUMBO-1 sequences,<sup>13</sup> can contribute to a significant increase in proton transverse coherence lifetimes  $T_2^H$  (corresponding to the refocused line width<sup>15</sup>).  $T_2^H$  as long as around 10 ms have been recently reported using those sequences.<sup>13</sup>

In this article we show that the use of these efficient line-narrowing techniques allows direct implementation of a solid-state version of refocused INEPT experiments for solids, which provides considerable improvement (up to a factor 3) over traditional through-bond MAS-J-HMQC<sup>4</sup> heteronuclear correlation methods at high MAS frequencies. We also show that performances of INEPT experiments can be further improved by direct application of the experimental optimization procedure<sup>16</sup> on the eDUMBO-1 decoupling scheme. This results in high-sensitivity INEPT experiments and opens up the way to a whole family of sequences that was previously inaccessible. We demonstrate the approach with an INEPT based Heteronuclear Single Quantum Correlation (HSQC) experiment applied to a microcrystalline sample of the protein Crh.

## 2. Solid-State INEPT Experiment

The pulse sequence for the solid-state refocused INEPT experiment for protonated solids is shown in Figure 1a. The original liquid-state technique<sup>9</sup> was adapted for rotating solids by adding proton homonuclear decoupling during the  $\tau$  and  $\tau'$  transfer periods, to remove proton–proton dipolar couplings. If the homonuclear decoupling is sufficiently efficient during those delays, fast magic-angle spinning then averages chemical shift anisotropy and heteronuclear dipolar couplings to zero, so that only the scalar couplings are preserved together with isotropic chemical shifts. The simultaneous 180° pulses on proton and carbon induce refocusing of isotropic chemical shifts after  $2\tau$  and  $2\tau'$ , such that during these delays only  $J_{CH}$  couplings affect coherence transfer and evolution (in addition to  $J_{CC}$  couplings in the case of <sup>13</sup>C-enriched compounds). For a pair of bonded (<sup>1</sup>H,<sup>13</sup>C) nuclei, after the first  $\tau$ – $\pi$ – $\tau$  period, antiphase proton coherence with respect to the attached carbon

is created, which is converted by the two simultaneous 90° pulses into antiphase carbon coherence. This antiphase <sup>13</sup>C coherence is then refocused during the second  $\tau'$ – $\pi$ – $\tau'$  period into observable carbon-13 magnetization. Note that the presence of proton homonuclear decoupling leads to effective scaled  $J_{CH}$  couplings, the scaling factor close to  $1/\sqrt{3}$  being specific to the employed decoupling scheme. In this work, decoupling of proton–proton dipolar interactions was achieved using several variants of the eDUMBO continuous phase modulation scheme,<sup>13</sup> as will be discussed further in the following.

Figure 1b shows the simulated behavior of the <sup>13</sup>C signal intensity while varying the  $\tau$  evolution delay for various refocused proton line widths  $\Delta'(^1\text{H})$ .<sup>17</sup> The so-called refocused line width is defined as the broadening observed indirectly in the proton dimension of a spin–echo experiment and corresponding to a characteristic refocused transverse dephasing time  $T_2^H$ .<sup>7,18</sup> Note that the refocused line widths are much smaller than the apparent proton line width  $\Delta$ , as has been discussed extensively in recent literature.<sup>13,15,17</sup> This is especially true under proton homonuclear decoupling, where differences of a factor 4 have been reported between the two.<sup>17</sup> The curves of Figure 1b, calculated for a  $J$  coupling of 130 Hz (which is a typical value for a one-bond  $J_{CH}$  coupling for sp<sup>3</sup> aliphatic carbons), are independent of carbon multiplicity, and the optimal  $\tau$  delay for proton evolution is predicted to be  $\tau = 1/4J_{CH}$ . When compared to an ideal liquid-state case with infinite proton effective transverse lifetime  $T_2^H = 1/\pi\Delta'(^1\text{H})$ , the maximum efficiency of <sup>1</sup>H–<sup>13</sup>C INEPT in solids under magic-angle spinning alone, simulated using  $\Delta'(^1\text{H}) = 500$  Hz, is shown to be extremely poor. Adding proton homonuclear decoupling during  $\tau$  delays considerably enhances the proton transverse coherence lifetimes. Values up to  $T_2^H \approx 10$  ms (corresponding to proton refocused line widths of  $\Delta'(^1\text{H}) = 30$  Hz; note that, in this case, apparent proton line widths of 130 Hz were obtained for CH<sub>3</sub> resonances) have been recently reported using eDUMBO-1<sub>22</sub> on a dipeptide sample.<sup>13</sup> This yields a significant improvement of the INEPT block transfer, and as shown in Figure 1b, 75% of the ideal transfer efficiency can be recovered under homonuclear decoupling conditions. Note that, for the solid-state cases, an effective  $J_{CH} = 75$  Hz was used which corresponds to a scaled value of the heteronuclear  $J$  coupling due to the presence of proton homonuclear decoupling. Figure 1c shows a similar type of curves featuring the <sup>13</sup>C signal intensity for a CH, CH<sub>2</sub>, and CH<sub>3</sub> group, as a function of the  $\tau'$  evolution delay for the ideal liquid-state case, with infinite carbon effective transverse lifetime  $T_2^C = 1/\pi\Delta'(^{13}\text{C})$ . Figure 1d presents the equivalent curves predicted for actual solid-state conditions using best available <sup>1</sup>H homonuclear decoupling,  $\Delta'(^{13}\text{C}) = 30$  Hz (corresponding to the full <sup>13</sup>C refocused line width at half-height of a single component in  $J$ -coupled multiplets). These carbon evolution curves show that careful choice of the  $\tau'$  delay should allow the use of the refocused INEPT experiment for spectral edition in solids. Perhaps more interesting, using rather short  $\tau'$  delays (around 1.3 ms in the solid-state case), it is also possible to acquire full <sup>13</sup>C spectra, where only carbons that are not directly bonded to protons are filtered out with an overall 65% efficiency compared to the ideal case for CH<sub>2</sub> resonances (accounting for relaxation from both

(14) Gerstein, B. C.; Pembleton, R. G.; Wilson, R. C.; Ryan, L. M. *J. Chem. Phys.* **1977**, *66* (1), 361–362. Gerstein, B. C. CRAMPS. In *Encyclopedia of NMR*; Grant, D. M., Harris, R. K., Eds. Wiley: Chichester, 1996; pp 1501–1509.

(15) De Paepe, G.; Lesage, A.; Steuernagel, S.; Emsley, L. *Chem. Phys. Phys. Chem.* **2004**, *5*, 869–875.

(16) De Paepe, G.; Hodgkinson, P.; Emsley, L. *Chem. Phys. Lett.* **2003**, *376* (3–4), 259–267.

(17) Lesage, A.; Duma, L.; Sakellariou, D.; Emsley, L. *J. Am. Chem. Soc.* **2001**, *123* (24), 5747–5752.

(18) Cowans B. A.; Grutzner J. B. *J. Magn. Reson. A* **1993**, *105* (1), 10–18.

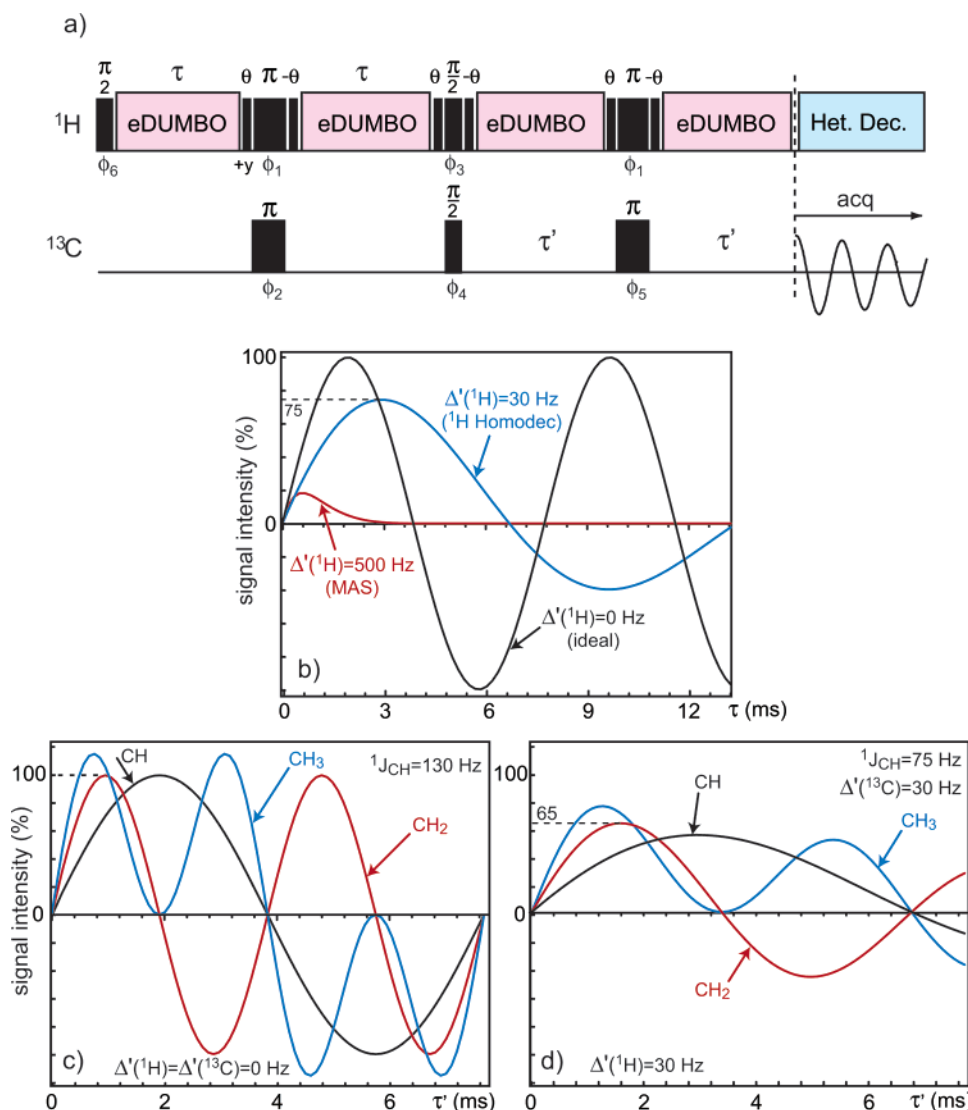


**Figure 1.** (a) Pulse sequence for the solid-state refocused INEPT experiment. The following 16-step phase cycle was used:  $\phi_1 = +x, -x$ ;  $\phi_2 = +x, -x$ ;  $\phi_3 = +y, +y, -y, -y$ ;  $\phi_4 = +x, +x, +x, +x, +y, +y, +y, +y, -x, -x, -x, -x, -y, -y, -y, -y$ ;  $\phi_5 = +x, -x, +x, +x, -x, +y, -y, +y, -y$ ;  $\phi_6 = +x, +x, +x, +x, +x, +x, -x, -x, -x, -x, -x, -x, -x, -x$ ; receiver =  $+x, +x, -x, -x, +y, +y, -y, -y$ . Theoretical curves for signal intensity observed on carbon-13 after the refocused INEPT block are shown in (b)–(d). Signal intensity is plotted in (b) as a function of  $\tau$  delay (evolution of  $^1\text{H}$  coherences), for  $^1\text{H}$  transverse dephasing times corresponding to: the ideal liquid-state case (black), and the solid-state cases with MAS only (red), and with  $\tau$  evolution under  $^1\text{H}$  homonuclear decoupling (blue). Carbon signal intensity is plotted as a function of the  $\tau'$  delay (evolution of  $^{13}\text{C}$  coherences) in (c) and (d) for different values of  $J_{\text{CH}}$  and  $\Delta' = 1/\pi T_2'$ , representative of the ideal liquid case (c) and the actual solid-state case (d). In (d), plotted signal intensities include a weight of 75% efficiency corresponding to the optimum  $\tau$  delay from (b). The curves follow theoretical behavior given by the following expressions: (for a CH group)  $\gamma_{\text{H}}/\gamma_{\text{C}} \sin(2\pi J_{\text{CH}}\tau) \sin(2\pi J_{\text{CH}}\tau') e^{-2\tau/T_2^{\text{H}}} e^{-2\tau'/T_2^{\text{C}}}$ ; (for  $\text{CH}_2$ )  $\gamma_{\text{H}}/\gamma_{\text{C}} \sin(2\pi J_{\text{CH}}\tau) \sin(4\pi J_{\text{CH}}\tau') e^{-2\tau/T_2^{\text{H}}} e^{-2\tau'/T_2^{\text{C}}}$ ; (for  $\text{CH}_3$ )  $3\gamma_{\text{H}}/4\gamma_{\text{C}} \sin(2\pi J_{\text{CH}}\tau) [\sin(2\pi J_{\text{CH}}\tau') + \sin(6\pi J_{\text{CH}}\tau')] e^{-2\tau/T_2^{\text{H}}} e^{-2\tau'/T_2^{\text{C}}}$ .

$^1\text{H}$  and  $^{13}\text{C}$  transverse coherences during  $2\tau$  and  $2\tau'$ ). For a fully  $^{13}\text{C}$ -labeled compound, due to the presence of  $J_{\text{CC}}$ , we expect to observe a shift of the optimal  $\tau$  and  $\tau'$  delays toward lower values, but without a dramatic loss in overall efficiency. This is illustrated in Figure 2 which shows calculated evolution curves of the signal intensity of a CH, a  $\text{CH}_2$ , and a  $\text{CH}_3$  carbon scalar-coupled to one or two neighboring spins using as a model the L-isoleucine spin system.

Figure 3 shows one-dimensional (1D) refocused INEPT spectra of a fully  $^{13}\text{C}$  labeled sample of L-isoleucine. According to the theoretical curves of Figures 1 and 2, the best intensity should be obtained for different  $\tau'$  values depending on the carbon multiplicity. In this study, we focus on the intensity of the  $\text{CH}_2$  resonance, since it is known to be the most difficult to decouple and thus the resonance that also provides the shortest

carbon and proton transverse coherence lifetimes under proton homonuclear decoupling; the optimal  $\tau$  and  $\tau'$  values giving the best signal for the  $\text{CH}_2$  resonance were found to be 0.9 ms. Figure 3a shows the 1D refocused INEPT spectrum acquired with very good sensitivity under high power eDUMBO-122 decoupling<sup>13</sup> ( $\nu_1 = 150$  kHz) and fast magic-angle spinning conditions ( $\omega_r = 22222$  Hz). (Note that the INEPT experiment is also practicable at lower MAS frequencies and lower homonuclear decoupling rf fields, for example,  $\omega_r = 12.5$  kHz and  $\nu_1 = 100$  kHz, which are conditions where DUMBO decoupling performs well.<sup>13,19</sup>) As expected, the  $^1\text{H}$ – $^{13}\text{C}$  INEPT filter very efficiently eliminates the  $^{13}\text{C}$  carboxyl resonance at 175.8 ppm. Figure 3b shows the results of application of the

(19) Lesage, A.; Sakellariou, D.; Hediger, S.; Elena, B.; Charmont, P.; Steuernagel, S.; Emsley, L. *J. Magn. Reson.* **2003**, *163* (1), 105–113.

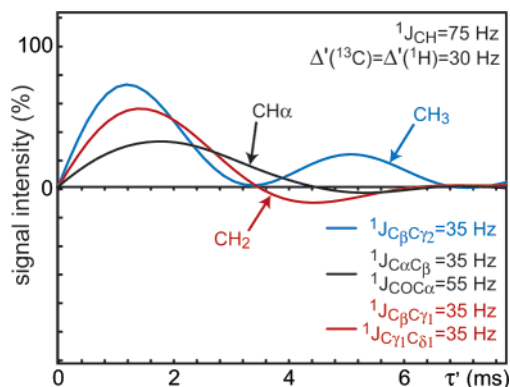


**Figure 2.** Theoretical curves for  $^{13}\text{C}$  signal intensity as a function of  $\tau'$  delay, plotted for the CH (black),  $\text{CH}_2$  (blue), and  $\text{CH}_3$  (red) resonances (same conditions as those in Figure 1d), in the case of a uniformly labeled compound. All relevant  $J_{CC}$  corresponding to the model case of  $[\text{U}-^{13}\text{C}]$ -L-isoleucine are included. Simulation was carried out using SIMPSON<sup>25</sup> with decay due to dephasing modeled by a simple exponential apodization of the curves.

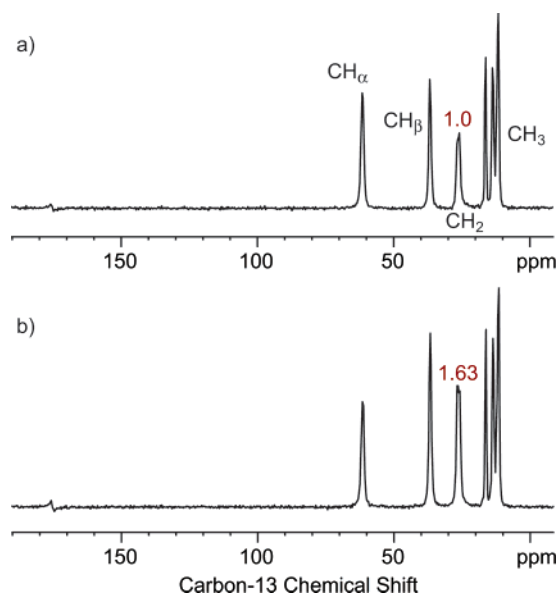


**Figure 3.** 125 MHz carbon-13  $[\text{U}-^{13}\text{C}]$ -L-isoleucine spectra (32 scans) acquired with the pulse sequence of Figure 1a, using eDUMBO-1<sub>22</sub> proton homonuclear decoupling during  $\tau$  and  $\tau'$  evolution (a), and after direct experimental optimization (targeting the maximum  $\text{CH}_2$  intensity) of the eDUMBO-1 sequence (b); the optimized phase modulation scheme is defined by Fourier coefficients  $\{a_n = 0$  (for all  $n$ );  $b_1 = 0.2150$ ,  $b_2 = 0.2114$ ,  $b_3 = 0.0563$ ,  $b_4 = 0.1559$ ,  $b_5 = 0.0015$ ,  $b_6 = 0.0468\}$ .  $\tau$  and  $\tau'$  delays were set to 0.9 ms, to give maximum intensity on the  $\text{CH}_2$  resonance. Experimental details are given in the text.

so-called experimental optimization procedure proposed recently,<sup>13,16</sup> where trial variants of eDUMBO-1<sub>22</sub> decoupling are directly tested on the spectrometer within an optimization loop. The peak height of the  $\text{CH}_2$  resonance in the 1D INEPT spectrum was taken as quality criterion for good homonuclear decoupling and optimum INEPT efficiency. The resulting spectrum presented in Figure 3b shows a gain of 63% in sensitivity for the  $\text{CH}_2$ , and the simplex optimization minimization converged in this case in less than an hour of optimization. It is important to remark that reoptimization is not necessary for each sample or session. The same parameters should be valid for similar samples (i.e., organic solids) and probes.

Figure 4 compares the efficiency and selectivity of the 1D  $^1\text{H}-^{13}\text{C}$  INEPT experiment with a standard high-power CP-

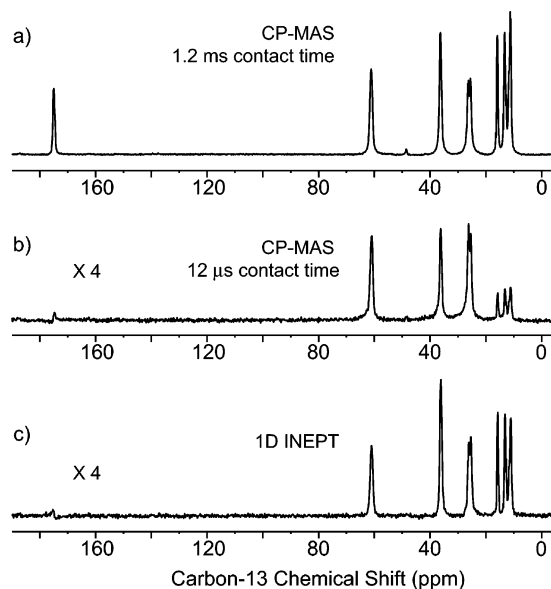


**Figure 4.** 175 MHz carbon-13 CP-MAS spectra of  $[\text{U}-^{13}\text{C}]$ -L-isoleucine (a–b), acquired with 1.2 ms (a) or 12  $\mu\text{s}$  (b) contact time, compared to the 1D INEPT spectrum (c) acquired with the optimized eDUMBO-1 decoupling scheme. High-power CP was implemented with rf frequencies  $\nu_C = 84$  kHz and average  $\nu_H = 94$  kHz (using a linear ramp of the amplitude from  $2/3$  to  $4/3$  of the average value). Other experimental details are given in the text. All spectra were acquired with the same number of scans.

MAS scheme. Long CP-MAS contact times obviously yield the best sensitivity but also invoke long range transfer and cannot be used usefully for HETCOR spectra. One-bond selectivity is obtained using short CP times, and in Figure 4b and c we compare short CP to INEPT. The selectivity in these 1D experiments can be assessed through the nonprotonated CO intensity (which corresponds also to the “best case scenario” for the performance of LG-CP type techniques). For equivalent selectivity (12  $\mu\text{s}$  contact time) we obtain similar overall sensitivity in Figure 4b and c with, as expected, a much more even intensity distribution with INEPT (as seen notably for  $\text{CH}_3$  groups) and the certainty that the transfer is through-bond. In both cases, about 20% intensity compared to a standard nonselective CP (1.2 ms contact time) is measured.

### 3. Experimental Section

The fully  $^{13}\text{C}$  enriched sample of L-isoleucine was purchased from Cambridge Isotope Laboratories and used without further recrystallization. All NMR experiments on this compound were performed at room temperature (293 K) on a Bruker Avance 500 WB spectrometer (500 MHz proton resonance frequency), equipped with a standard 2.5 mm double-tuned MAS probe, except experiments described in Figure 4 acquired on a Bruker Avance 700 SB spectrometer equipped with a 3.2 mm triple-tuned MAS probe. Approximately 10 mg of sample were used. The MAS spinning frequency was set to 22 222 Hz. During heteronuclear transfer delays ( $\tau$  and  $\tau'$  which were synchronized with the rotor period), eDUMBO-1 proton homonuclear decoupling was implemented with a radio frequency field strength of  $\nu_1 = 150$  kHz. Each decoupling cycle ( $\tau_C = 20$   $\mu\text{s}$ ) was divided into 50 phase steps of 400 ns each. The overall phase of eDUMBO-1 decoupling was adjusted to make the effective decoupling field lie in the ( $x$ ,  $z$ ) plane. The short  $\theta$  pulses (0.5  $\mu\text{s}$ ) rotate magnetization back into the ( $x$ ,  $y$ ) plane from the evolution plane which is perpendicular to the decoupling field. Conversely, the “ $-\theta$ ” pulses rotate magnetization from the ( $x$ ,  $y$ ) plane to the effective evolution plane during proton homonuclear decoupling. Misadjustment of the length of the  $\theta$  pulses results in

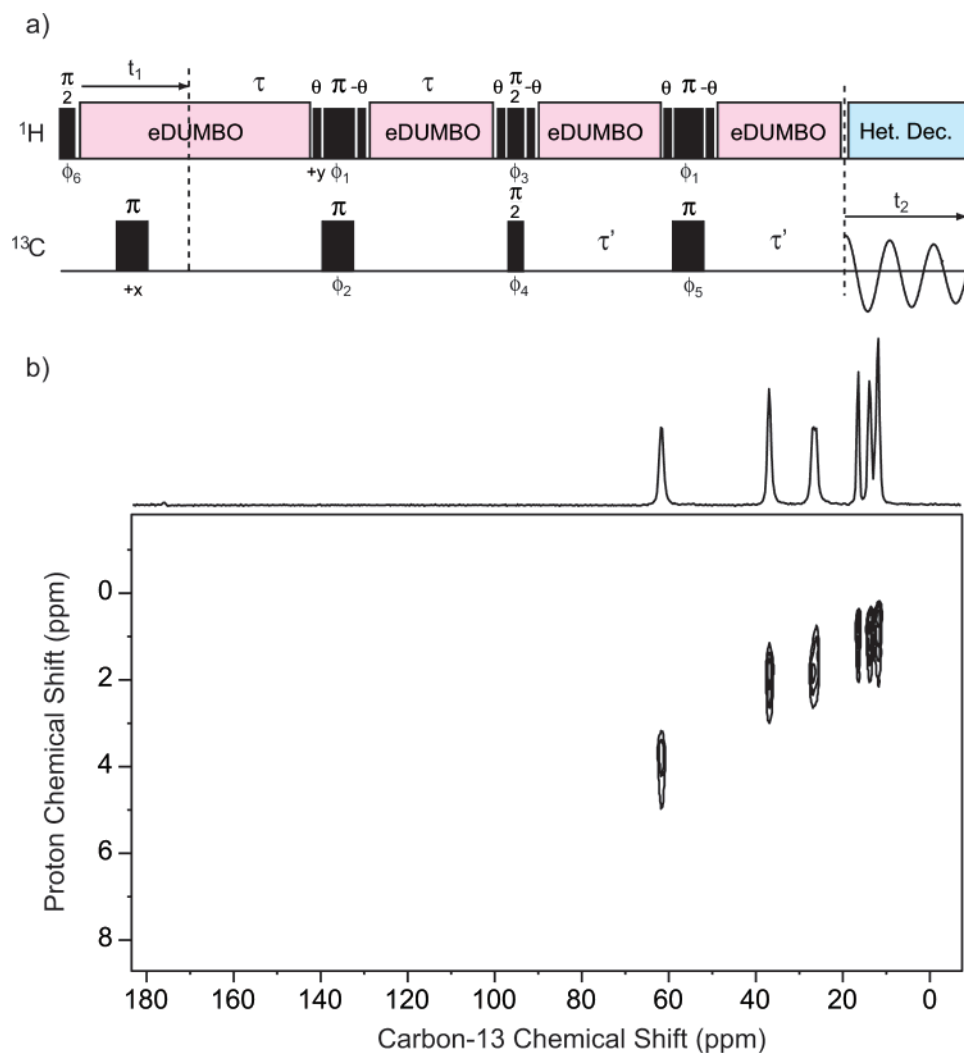


**Figure 5.** Pulse sequence for the 2D INEPT HSQC experiment (a), and corresponding 125 MHz carbon-13 spectrum of [U-<sup>13</sup>C]-L-isoleucine (b).  $\tau$  and  $\tau'$  delays were set to 0.9 ms, to produce maximum intensity on the CH<sub>2</sub> resonance. 32 scans were acquired with 80  $\mu$ s  $t_1$  increments, corresponding to a maximum  $t_1$  evolution period of 12.8 ms, and a recycle delay of 3 s, for a total experimental time of 8 h 40 min. The optimized eDUMBO-1 decoupling scheme has been used in both the excitation,  $t_1$  evolution and reconversion delays. Other experimental details are given in the text.

appearance of axial peaks in the 2D INEPT spectra. Note that, in most experiments, we cannot completely remove the axial peaks for all resonances simultaneously. The TPPM heteronuclear decoupling was applied during <sup>13</sup>C acquisition with a proton nutation frequency  $\nu_1 = 100$  kHz.<sup>20</sup> The 180° pulse lengths on proton and carbon were set to 5  $\mu$ s. A 16-step phase cycle was used to select the proper coherence pathway for the refocused INEPT transfer. Thus, for experimental optimization on 1D spectra, 16 transients were coadded to acquire a complete phase cycle. For 2D INEPT based HSQC experiments, quadrature detection in F<sub>1</sub> was achieved using the TPPI method<sup>21</sup> on the first proton 90° pulse. The [U-<sup>13</sup>C,<sup>15</sup>N] labeled Crh protein sample was prepared as described previously.<sup>22</sup> The INEPT HSQC experiment on microcrystalline Crh was recorded at 700 MHz for protons, using a standard-bore 3.2 mm triple resonance MAS probe with a spinning frequency of 22 kHz. The temperature of the sample was regulated at 259 K, corresponding to an actual sample temperature of about 5 °C. Other experimental details are given in the caption of Figure 7. In the F<sub>1</sub> dimension of 2D spectra, proton chemical shifts were corrected by applying a scaling factor of 0.57 as determined experimentally from a

<sup>1</sup>H spectrum of L-alanine recorded under similar homonuclear decoupling conditions. All pulse programs and phase cycles are available from our website<sup>23</sup> or by request to the authors.

#### 4. Discussion

Besides potential applications of 1D refocused INEPT experiments to spectral editing or to the measurement of  $J_{CH}$  couplings in solids, its application to multidimensional spectroscopy opens up a plethora of possibilities and notably provides, in one of the most simple incarnations, a very competitive method for selective one-bond 2D HSQC spectroscopy. Figure 5a describes the pulse scheme for the acquisition of 2D <sup>1</sup>H-<sup>13</sup>C through-bond correlation spectra using refocused INEPT transfer. Similarly to the 1D solid-state INEPT experiment of Figure 1a, this pulse scheme was directly inspired from liquid-state NMR methodology.<sup>24</sup> Figure 5b shows a 2D spectrum acquired for [U-<sup>13</sup>C]-L-isoleucine with this pulse sequence, and Figure 6 evaluates the comparative efficiency of the experiment. The 2D

(20) Bennett, A. E.; Rienstra, C. M.; Auger, M.; Lakshmi, K. V.; Griffin, R. G. *J. Chem. Phys.* **1995**, *103* (16), 6951–6958.

(21) Marion, D.; Wuthrich, K. *Biochem. Biophys. Res. Commun.* **1983**, *113* (3), 967–974.

(22) Bockmann, A., et al. *J. Biomol. NMR* **2003**, *27* (4), 323–339.

(23) <http://www.ens-lyon.fr/CHIMIE>.

(24) Bax, A.; Morris, G. A. *J. Magn. Reson.* **1981**, *42* (3), 501–505.

(25) Bak, M.; Rasmussen, J. T.; Nielsen, N. C. *J. Magn. Reson.* **2000**, *147* (2), 296–330.

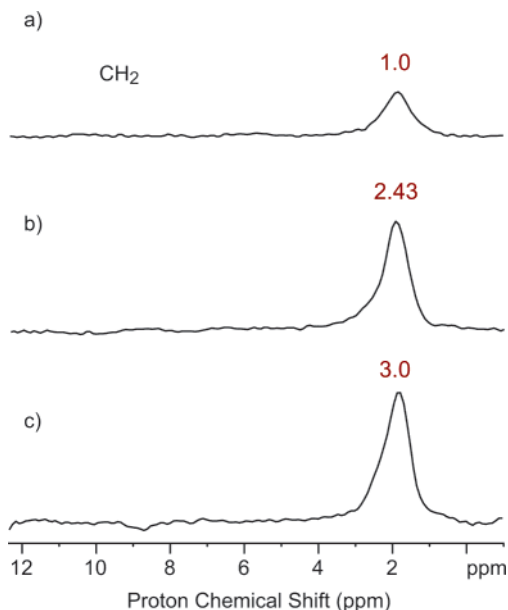


**Figure 6.** Slices parallel to  $F_1$  extracted from 2D heteronuclear correlation spectra at the  $\text{CH}_2$  carbon resonance frequency (26.1 ppm) of  $[\text{U}-^{13}\text{C}]\text{-L}$ -isoleucine. The efficiency of the standard 2D MAS-J-HMQC experiment (a) is compared with the 2D INEPT HSQC experiment in (b) and (c) corresponding to pulse sequence and experimental conditions of Figure 5, respectively, using eDUMBO-1<sub>22</sub> proton homonuclear decoupling (b) or its experimentally optimized variant (c) described in Figure 3. For 2D MAS-J-HMQC experiment, the  $\tau$  evolution delay was set to 1.8 ms and eDUMBO-1<sub>22</sub> homonuclear decoupling was used.

MAS-J-HMQC<sup>4</sup> considered as the state-of-the-art through-bond heteronuclear correlation method was chosen as a reference for comparison with the 2D INEPT method proposed here. (The comparison with short CP dipolar transfer is provided in Figure 4.) Again, the  $\text{CH}_2$  resonance is known to be the most difficult one to observe in a 2D correlation spectrum, and Figure 6 shows slices parallel to  $F_1$  that were extracted from 2D data for this particular resonance. The apparent proton line widths  $\Delta(^1\text{H})$  obtained in this sample under our experimental conditions are about 385 Hz (0.77 ppm) for  $\text{CH}_2$  and 210 Hz (0.42 ppm) for

$\text{CH}_3$  protons. The refocused line widths  $\Delta'(^1\text{H})$  have not been measured in this particular sample, but as mentioned above, large differences are expected between  $\Delta$  and  $\Delta'$ . A major enhancement compared to the 2D MAS-J-HMQC is obtained with the 2D INEPT method, up to a factor of 3 when using the directly optimized eDUMBO-1 scheme obtained previously from the 1D refocused INEPT. Significant sensitivity improvements are also observed for all other resonances present in the 2D spectrum. It is worth noting that all the parameters, in particular the  $\tau$  and  $\tau'$  delays, have been chosen to maximize intensity of the  $\text{CH}_2$  peaks and that a different set of parameters can yield a greater sensitivity for aliphatic resonances that have a different multiplicity, especially for the  $\text{CH}_3$  groups.

It is worth noting that for natural abundance samples the INEPT based sequence does not yet improve on the sensitivity of the MAS-J-HMQC experiment. This can be rationalized since for fully labeled compounds the MAS-J-HMQC sequence suffers from the presence of  $J_{\text{CC}}$  couplings in both the excitation and reconversion blocks, leading to an attenuation of the signal. This is generally the case for sequences involving extended evolution of carbon coherences and highlights the intrinsic advantage of INEPT in isotopically enriched systems. In addition, in the MAS-J-HMQC experiment, magnetization is first transferred from proton to carbon spins through a long cross-polarization step, which yields a larger enhancement in natural abundance compounds than in uniformly  $^{13}\text{C}$ -labeled samples (due to the higher proton to carbon-13 ratio). In natural abundance compounds the advantage of INEPT is thus slightly lessened, but we nevertheless obtain similar sensitivity as for the previous schemes (i.e., there is no disadvantage to INEPT, and the other advantages to this approach are maintained).

Finally, it is interesting to probe the practicability of the presented 2D  $^1\text{H}$ - $^{13}\text{C}$  INEPT HSQC technique for studying complex systems. Figure 7 shows such an example with data recorded on a sample of microcrystalline Crh,<sup>22</sup> 85-residue *Bacillus subtilis* protein involved in catabolite repression. We note that this high-quality HSQC spectrum can be obtained straightforwardly with good sensitivity in a reasonable experi-

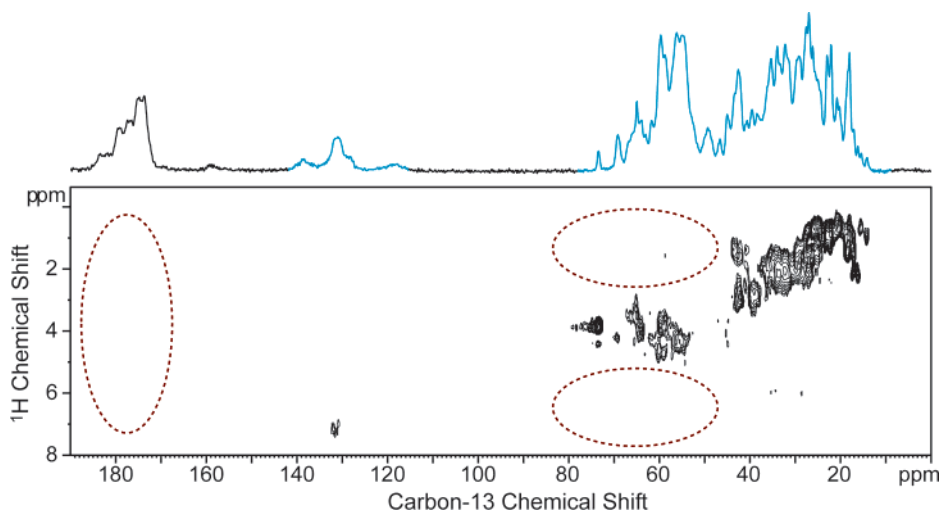


**Figure 7.** Two-dimensional 700 MHz proton frequency  $^1\text{H}$ - $^{13}\text{C}$  INEPT HSQC spectrum of microcrystalline Crh, recorded with the pulse sequence shown in Figure 5a at  $\omega_{\text{R}} = 22$  kHz. 192 transients were collected for each  $t_1$  point (128  $\mu\text{s}$  increment) with a recycle delay of 3 s. Total experimental time was 21 h. During  $t_1$  and INEPT evolution delays ( $\tau = \tau' = 448$   $\mu\text{s}$ ), eDUMBO-1<sub>22</sub> proton homonuclear decoupling was applied with  $\nu_1 = 100$  kHz (32  $\mu\text{s}$  decoupling cycle time). For  $^{13}\text{C}$  detection, TPPM heteronuclear decoupling was used with  $\nu_1 = 80$  kHz. One-dimensional  $^{13}\text{C}$  CP-MAS is shown for comparison on top of the 2D data. Blue lines correspond to regions of the spectra containing protonated carbon resonances. The red dotted circles correspond to regions that would contain two-bond correlations.

mental time (here 21 h). Particularly, we observe excellent *selectivity* for both the 1D and 2D INEPT data with respect to the carbonyl resonances or the potential two-bond transfers in the aliphatic region (peaks which would appear in the red circled regions on the figure), *which are completely absent* in the 2D spectrum. This kind of selectivity is difficult to obtain with other methods.

## 5. Conclusion

In conclusion, we have shown that standard refocused INEPT methodology from liquid-state NMR can be successfully transferred to solid-state spectroscopy, when combined with efficient proton homonuclear dipolar decoupling schemes under fast magic-angle spinning conditions. The 2D INEPT method is shown to provide significantly improved through-bond HSQC spectra with respect to previous through-bond methods, which are in themselves of major interest for the characterization and assignment of solid-state systems. A sensitivity improvement of a factor three was observed for fully  $^{13}\text{C}$ -labeled L-isoleucine. The overall sensitivity improvement is such that with this through-bond method sensitivity is now comparable to dipolar

through-space methods using short CP times. This experiment could prove to be very useful in the case where the protons are isotopically diluted and where the lower ratio of protons to carbons leads to a reduced efficiency of dipolar HETCOR experiments in solids. Another important application will involve systems where local dynamics partly average out the dipolar couplings. The feasibility of using the INEPT transfer block has been demonstrated here for ( $^1\text{H}$ ,  $^{13}\text{C}$ ) pairs of spins but should be also practicable to obtain through-bond ( $^1\text{H}$ ,  $^{15}\text{N}$ ) correlations. Apart from the improved sensitivity in enriched compounds, most interesting is probably the potential now to use the INEPT through-bond transfer building block in more sophisticated correlation schemes, and this is under development in our laboratory. The key factor here is that this allows, for the first time, evolution of proton transverse coherence during  $\tau$  periods in solids, which was previously prohibitive. Notably, this polarization transfer scheme could greatly contribute to the efficiency of proton detected multidimensional correlation experiments in solids.

JA054411X